Electronic Supporting Information

Making more from Bio-Based Platforms: Life Cycle Assessment and Techno-Economic Analysis of *N*-Vinyl-2-Pyrrolidone from Succinic Acid

Moritz O. Haus[‡,a], *Benedikt Winter*[‡,b,c], *Lorenz Fleitmann* [b,c], *Regina Palkovits*[*,a] *and André Bardow*[*,b,c,d]

[a] Chair of Heterogeneous Catalysis and Technical Chemistry, RWTH Aachen University, Worringerweg 2, DE-52074 Aachen. E-Mail: palkovits@itmc.rwth-aachen.de

[b] Energy and Process Systems Engineering, ETH Zurich, Tannenstraße 3, CH-8092 Zurich. E-Mail: abardow@ethz.ch

[c] Institute of Technical Thermodynamics, RWTH Aachen University, Schinkelstraße 8, DE-52062 Aachen.

[d] Institute of Energy and Climate Research (IEK 10), Research Center Jülich GmbH, Germany

[‡] These authors contributed equally to this work.

[*] Corresponding authors

TABLE OF CONTENTS

1. Experimental Laboratory Procedures

The hydrogenation-amidation of succinic acid and the purification of respective products is established in laboratory practice only. Thus, a small experimental dataset was collected to underline the soundness of process proposals given in the main text. Respective materials, methods and procedures are as follows:

Chemicals. *N*-(2-hydroxyethyl)-2-pyrrolidone (HEP, 98 %), *N*-methyl-2-pyrrolidone (NMP, anhydrous, ≥99.5 %), 2-pyrrolidone (2PYD, 99 %), succinic acid (≥99 %), γ-butyrolactone (GBL, ≥99 %), monoethanolamine (MEA, ≥99 %), trimethylsilyl chloride (TMSCl, ≥98%), acetonitrile (99.8 %), $Pt(NH_3)_4(NO_3)_2$ (≥50 wt.% Pt) and 5 wt.% ruthenium on activated carbon (Ru/C) were sourced from Sigma Aldrich. Other chemicals were purchased as follows: *N*-ethyl-2-pyrrolidone (NEP, 98 %) from abcr, *N,O*-bis(trimethylsilyl)trifluoroacetamide (BSTFA, 98 %) from J&K, mesitylene (98%) from Acros Organics, dichloromethane (DCM, ≥99.9 %) from ChemSolute, NH_4ReO_4 (>99.5 %) from ChemPur, TiO_2 (ST6*120) from Saint-Gobain NorPro, Hydranal™-Composite 5 from Honeywell, Hydranal™ Methanol Rapid from Fluka.

Pt-Re catalyst. The bimetallic Pt-Re/TiO_2 catalyst was developed in another study.[1] Its preparation followed the "layer deposition (LD)" technique. $Pt(NH_3)_4(NO_3)_2$ and NH_4ReO_4 were used as metal precursors. The support material, anatase TiO_2, was ground and sieved (<180 µm) prior to use.

Test reactions for the conversion of succinic acid/GBL to HEP were performed in batch mode and according to previously disclosed procedures.[1,2] In a typical recipe, 1.5 g of succinic acid were reacted with one molar equivalent of monoethanolamine, using 1.5 g H_2O as a solvent and 37.5 mg of catalyst. Typical reaction temperatures and initial pressures were set at 150-200°C and 150 bar

H_2. For experiments on γ-butyrolactone as alternative substrate, succinic acid in the above recipe was replace by an equivalent molar quantity of GBL.

Irrespective of substrate, the liquid reaction products were analyzed by HPLC (Organic Acid Resin column, Chromatography Services) and GC (50 m Rtx-Pona, ID-0.25 mm + DF-0.5µm) after filtration (polyamide syringe filter). While HPLC analysis required dilution with deionized water, GC analysis required silylation of analytes prior to the measurement. This was performed by adding 20 mg of sample to 2 mL of a silylation agent consisting of BSTFA, TMSCl, mesitylene (GC standard) and acetonitrile (4:1:0.25:5 volume parts). The mixture was left to react in a closed glass vessel suspended in an ultrasonication bath at 60 °C for 2 h. The following definitions for conversion (X) and yield (Y_i) were applied to obtain respective figures from chromatographically determined concentrations (c_i) and molar quantities (n_i):

$$X = 1 - \frac{\sum_{i=\text{not reduced}} n_i}{n_{\text{substrate}(t=0)}} \quad (1)$$

(X excludes non-catalytic, thermal reactions, such as amide formation.)

$$Y_i = \frac{n_i}{n_{\text{substrate}(t=0)}} \quad (2)$$

$$c_{\text{org,Chrom}} = \sum_{i=\text{species quant. in chrom.}} c_i \quad (3)$$

Additionally, the water fraction ($c_{H2O,KF}$, g g^{-1}) in each liquid sample was determined by automated Karl Fischer-titration on a Titroline® 7500 KF (SI Analytics) using Hydranal™-Composite 5 and Hydranal™ Methanol Rapid reagents. Samples were measured twice in succession with relative deviations staying below ±2 %. Thus, the total concentration of organics after the reaction ($c_{org,KF} = 1\text{-}c_{H2O,KF}$) could be compared to that of all species quantified in chromatography ($c_{org,Chrom}$, g g^{-1}).

Separation experiments. Vacuum distillations (0.03 mbar) were performed in batch mode, using a glass microdistillation setup with a 3 cm Vigreux column. The distillation bottoms were heated by an oil bath and product collection flasks were suspended in ice water. The main product fraction for further analysis was obtained at 110 °C (head temperature). Some organic residue remained in the distillation bottoms even at the maximum oil bath temperature (195 °C).

Batch extractions were performed with dichloromethane (DCM) due to the pronounced polarity of most reaction products. One part (volume) of the aqueous reaction solution was vigorously mixed with three parts of DCM in an extraction funnel. The heavy organic phase was collected after a settling period. The remaining aqueous phase was used for another four extraction cycles, each with fresh DCM solvent. All five organic extracts were mixed and dried with $MgSO_4$. Subsequent removal of DCM on a rotary evaporator led to the final sample extract.

2. Experimental Results on Amidation-Hydrogenation

a. Mass Balances for Process Simulation

The mass balance of amidation-hydrogenation was first evaluated in a kinetic test experiment with Ru on carbon (Ru/C) as catalyst (**Figure S1**). At low and modest conversion, the total organic content of reaction samples determined by Karl Fischer-titration ($c_{org,KF}$) agreed well with the sum of species concentrations determined by chromatography ($c_{org,Chrom}$). Thus, all significant products formed in this stage of the reaction lend themselves to chromatographic quantification. The total error of the method is capped at ±5 wt.% as is evident from the analysis of samples derived in the absence of catalyst (Figure S1, purple dots). With increasing conversion over Ru/C, the fraction of organics identified by chromatography starts to decline, causing a significant gap in the overall

mass balance. Thus, 14.4 wt.% of total organics are not accounted for by chromatography once full conversion is approached (24 h reaction). Notably, this measure relates to the liquid sample only and is therefore not affected by low levels of ethane and methane production that were previously reported for the amidation-hydrogenation of succinic acid.[2]

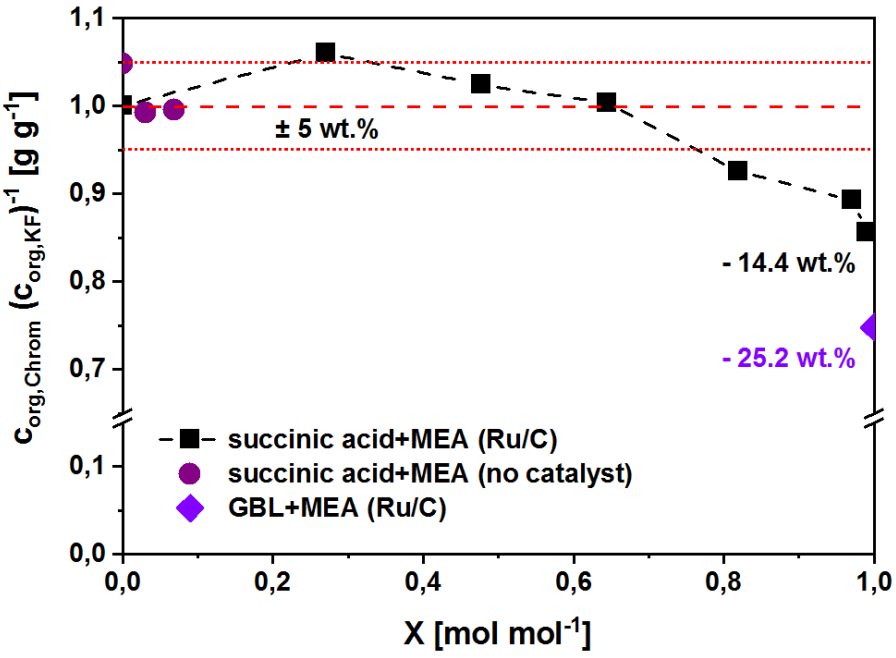

Figure S1: Oligomer formation as a function of reaction conditions measured by Karl Fischer-titration and chromatography. (Conditions: 200 °C, 150 bar H_2, 750 rpm, 37.5 mg Ru/C, where catalyst was added)

The failure of chromatographic analysis is assigned to the high boiling point (GC) and strong adsorption properties (HPLC) of the unidentified compounds. Oligomerization is seen as their likely origin, due to the presence of multiple condensable functionalities within the reaction mixture. Accordingly, an extension of the previously presented reaction network[2] of succinic acid amidation-hydrogenation is given in **Figure S2**. Therein, succinic acid reacts with MEA to give amides and imides, which are then hydrogenated into the target product HEP (*N*-(2-hydroxyethyl)-2-pyrrolidone). Depending on the catalyst's selectivity towards C-O vs. C-N hydrogenolysis,

N-(2-hydroxyethyl)-4-hydroxybutanamide (HEBA) is observed as an alternative product. However, intramolecular condensation to HEP limits HEBA levels in reaction samples derived at T > 150 °C.[3] Pure succinic acid hydrogenation and sequential HEP reduction are of greater concern, since respective products (e.g. 1,4-butandiol, *N*-methyl-2-pyrrolidone) are without use in NVP production. The same applies to the oligomeric fraction, which is likely formed from a reduced intermediate due to its appearance at high conversion.

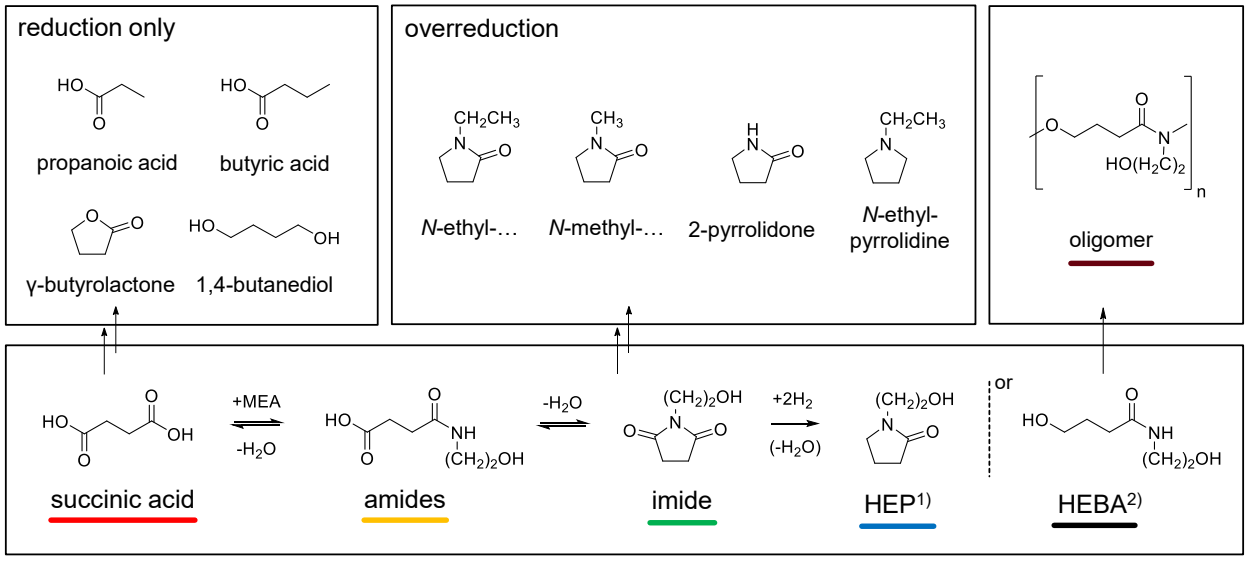

Figure S2: Extended reaction network of succinic acid amidation-hydrogenation, including oligomer formation and undesired reductions. 1) *N*-(2-hydroxyethyl)-2-pyrrolidone, 2) *N*-(2-hydroxyethyl)-4-hydroxybutanamide.

Interestingly, oligomer formation was previously reported by other authors[3,4] dealing with similar reaction systems. Most notably, Shimasaki et al. suggested reversible oligomer formation from several HEBA units.[3] This is underlined by a high fraction of unknown organics (~25 wt.%) in reactions starting directly from γ-butyrolactone and MEA (Figure S1). These substrates are known to react quantitatively, yielding high levels of HEBA in the initial reaction stages. In the case of amidation-hydrogenation, depolymerization of oligomers may be suppressed through sequential hydrogenation steps.

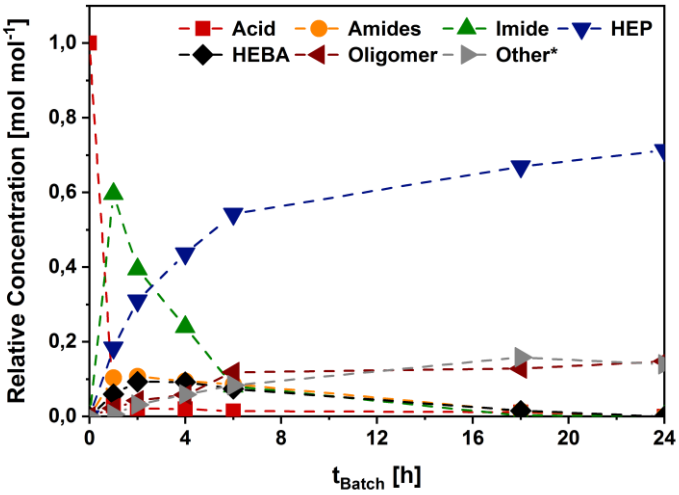

Figure S3: Concentration-time-profile of succinic acid amidation-hydrogenation. Oligomer contents based on Karl Fischer-titration are included. *products from pure hydrogenation and overreduction, such as NMP and butanols. (Conditions: 200 °C, 150 bar H_2, 750 rpm, 37.5 mg Ru/C)

Given the above, the gap between Karl Fischer-titration and chromatographic analysis serves as estimate of the oligomeric fraction within the reaction product. Thus, closed mass balances, which are essential for process modelling, could be obtained. An exemplary concentration-time-profile of succinic acid amidation-hydrogenation, including oligomer formation, is given in **Figure S3**.

b. Influence of the Catalyst System

Since high conversions and HEP yields are obtainable in amidation-hydrogenation, substrate recycle was not considered for process modelling. Instead, the reactor models were based on high conversion experiments from batch catalyst testing (**Table S1**). In this context, previously proposed hydrogenation catalysts lead to variable outcomes. Most notably, an optimized bimetallic system (Pt-Re/TiO_2) leads to higher HEP yield as compared to the commercial Ru/C benchmark. The higher yield is mostly due to the suppression of oligomer formation and sequential HEP

reduction. Further details are given elsewhere.[1] To quantify the potential for further catalyst development, both catalyst options are compared to an idealized material, characterized by 98 % HEP yield and minor by-product formation.

Table S1: Detailed summary of reaction results implemented in process models for bio-based NVP production. (Conditions: 200 °C, 150 bar H_2, 24 h, 750 rpm, 37.5 mg catalyst)

	$n_i/n_{substrate,0}$ [mol mol^{-1}]		
Substrate/Product (i)	**Ru/C**	**Pt-Re/TiO$_2$**	**ideal**
HEP	**0.713**	**0.830**	**0.98**
N-ethyl-…	0.020	0.028	0
N-methyl-…	0.058	0.006	0
2-pyrrolidone	0.010	0.014	0.01[b]
N-ethylpyrrolidine	0.007	0.000	0
GBL	0.012	0.000	0
1,4-butanediol	0.013	0.019	0
butyric acid	0.005	0.012	0
propanoic acid	0.014	0.000	0
oligomer[a]	0.148	0.082	0.01[b]

[a] defined as the gap between chromatographic analysis and Karl Fischer titration; given in moles of repetitive C4 units. [b] even an optimized future catalyst is likely to yield some by-products.

c. Experimental Oligomer Separation

The separation of oligomer from light-boiling reaction products was tested in lab-scale vacuum distillation and extraction. The success of these methods can be judged by the fraction of identified organics (chromatography vs. Karl Fischer titration) in samples before and after purification (**Figure S4**). It is observed that, within the error of the analysis (± 5 %), distillate and extract fractions are free of unidentified oligomers, which instead accumulate in the distillation bottoms and the raffinate. Thus, both approaches to HEP purification are deemed functional.

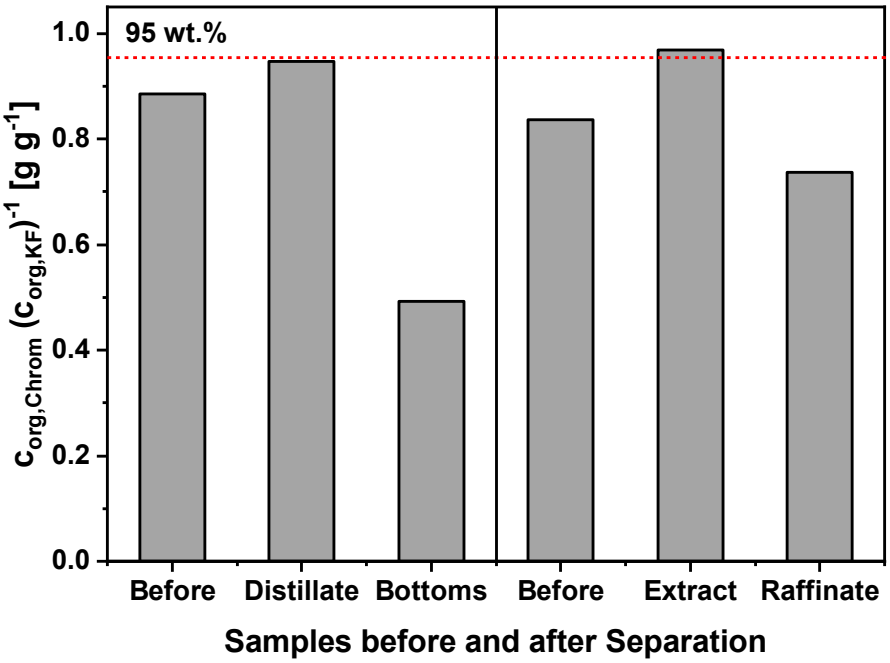

Figure S4: Impact of separation strategies on the identified fraction of organics in reaction samples. Both initial samples are derived from high conversion experiments. (Reaction conditions: 200 °C, 150 bar H_2, 24 h, 750 rpm, 37.5 mg Ru/C)

Notably, the levels of vacuum applied in laboratory distillations are not easily available on the industrial scale. As a result, higher bottoms temperature would have to be implemented, potentially leading to issues associated with thermal instability of chemicals. Extraction, on the other hand, does not suffer from these constraints and will thus have a higher chance of success in upscaling. It is considered be a more conservative approach to oligomer separation.

3. Life Cycle Inventories

a. LCIs of literature-reported process steps

Life cycle inventories for the conversion of succinic acid to NVP were derived from process simulations, while data on previous steps towards succinic acid is taken from literature. Here, **Table S2**, **Table S3** and **Table S4** give an overview of LCIs for succinic acid production from sugar beet. For analogue data sets on other biomass feedstocks, the reader is referred to Winter et al.[5]

Table S2: LCI for agricultural sugar beet production. (adopted from Winter et al.[5])

Input			Output		
Name	**Quantity**	**Unit**	**Name**	**Quantity**	**Unit**
Chemicals/Materials			*Emissions (Air)*		
N-Fertilizer	2.26	g	N_2O	0.14	g
P_2O_5	0.85	g	NO_x	0.38	g
K_2O	1.24	g	NH_3	0.06	g
Fuels/Energy			*Emissions (Water)*		
Diesel	0.17	MJ	NO_3^-	0.63	g
			P	0.05	g
			Product		
			Sugar beet	1.0	kg

Table S3: LCI for glucose production from sugar beet. (adopted from Winter et al.[5])

Input			Output		
Name	**Quantity**	**Unit**	**Name**	**Quantity**	**Unit**
Chemicals/Materials			*Products*		
Sugar beet	6.50	kg	Glucose	1.0	kg
Limestone	0.15	kg	Beet pulp	0.65	kg
Gypsum	6.90	g	Calcium carbonate	0.30	kg
Sulphuric acid	1.10	g			
Formaldehyde	0.98	g			
Sulphur dioxide	0.85	g			
Sodium carbonate	0.33	g			
Hydrochloric aicd	0.16	g			
Fuels/Energy					
Natural gas	2.19	MJ			
Coke	0.33	MJ			
Electricity	0.21	kWh			

Table S4: LCI for succinic acid production by low-pH yeast fermentation of glucose. (adopted with modification from Cok et al.[6])

Input			Output		
Name	**Quantity**	**Unit**	**Name**	**Quantity**	**Unit**
Chemicals/Materials			*Product*		
Glucose	1.35	kg	Succinic acid	1.0	kg
Process water	31	kg			
Hydrochloric acid	0.128	kg			
Fuels/Energy					
Natural gas	9.93	MJ			
Electricity	0.60	kWh			

Table S5: LCI for succinic acid production by fermentation of glucose. (adopted with modification from Adom et al.[35])

Input			Output		
Name	**Quantity**	**Unit**	**Name**	**Quantity**	**Unit**
Chemicals/Materials			*Product*		
Glucose	1.90	kg	Succinic acid	1.0	kg
Fuels/Energy					
Natural gas	17	MJ			

b. Heterogeneous catalysts in *Bio* scenario LCIs

While heterogeneous catalysts are not consumed according to ideal definitions, deactivation typically limits their useful lifetime. Thus, a small amount of the heterogeneous catalysts must be considered within the LCIs of *Bio* scenarios. More precisely, this amount can be defined through the quantity of substrate converted per $kg_{Catalyst}$ prior to material exchange, i.e. catalyst stability expressed as a turnover number.

Due to the nature of the presented evaluation, information on the long-term stability of heterogeneous catalysts in *Bio* scenarios was not available. However, during lab-scale experiments, the Na_2O/SiO_2 HEP dehydration catalyst was able to convert 96 kg_{HEP} kg_{Cat}^{-1} without showing signs of deactivation (8 h operation).[2] Related literature also suggests that catalyst activity can be easily restored by calcination, when reduced conversion is observed.[3] Thus, it is assumed that Na_2O/SiO_2 reaches a minimum turnover of 500 kg_{HEP} kg_{Cat}^{-1} before requiring replacement.

For amidation-hydrogenation catalysts, experiments have demonstrated stability over five batch experiments, equating to the conversion of max. 200 kg_{Acid} kg_{Cat}^{-1} over 120 h operation time (assuming 24 h experiments to reach full conversion).[2] In the absence of long-term stability test results, turnover of 2,000 kg_{Acid} kg_{Cat}^{-1} is assumed prior to catalyst exchange in process evaluation

(= 1,200 h time on stream). Notably, lifetimes of similar materials have previously been estimated at between five and ten years (8000 h yr^{-1}), wherefore our analysis leans to the conservative side.[7] In the case of Pt-Re/TiO_2, a transition to continuous reactor types during process upscaling may be required to reach this extent of stability.[1]

4. Life Cycle Impact Assessment

a. LCIA background processes

Table S6: Summary of database background processes used in the evaluation of LCIs.

Input/Output stream	Background process
Succinic acid-based NVP (Chemicals)	
Hydrogen	DE: Hydrogen (steam reforming from natural gas) ts
Dichloromethane	DE: Dichloromethane ts
Nitrogen	DE: Nitrogen (gaseous) ts
Process water (deionized)	EU-28: Process water ts
Silica (catalyst)	DE: Silica sand (flour) ts
Sugar fermentation (Chemicals)	
Hydrochloric acid	DE: Hydrochloric acid mix(100%) ts
Water	DE: Water (desalinated)
Monoethanolamine (Chemicals)	
Ethylene oxide	DE: Ethylene oxide (EO) via air ts
Ammonia	DE: Ammonia (NH3) without CO2 recovery (carbon dioxide emissions to air) ts
GBL-based NVP (Chemicals)	
Ammonia	DE: Ammonia (NH3) without CO2 recovery (carbon dioxide emissions to air) ts
Potassium hydroxide	RER: potassium hydroxide production ecoinvent 3.6
Acetylene	DE: Ethine (acetylene) ts
Process water (deionized)	EU-28: Process water ts

GBL from Maleic anhydride (Chemicals)	
Maleic anhydride	DE: Maleic anhydride ts
Hydrogen	DE: Hydrogen (steam reforming from natural gas) ts
Sodium hydroxide	DE: Sodium hydroxide (caustic soda) mix (100%) ts
Fuels/Energy	
Natural gas	DE: Thermal energy from natural gas ts
Steam	DE: Process steam from natural gas 90% ts
Refrigerant	DE: Electricity grid mix ts
Cooling water	Cut-off (minor contribution)
Air cooling	Cut-off (minor contribution)
Electricity	DE: Electricity grid mix ts
Pt/Ru (in catalyst) by allocation	
	RER: blasting ecoinvent 3.3
	RER: chemical factory construction, organics ecoinvent 3.3
	GLO: chemical production, inorganic ecoinvent 3.3
	GLO: chemical production, organic ecoinvent 3.3
	RER: conveyor belt production ecoinvent 3.3
	RER: hydrogen cyanide production ecoinvent 3.3
	GLO: market for mine infrastructure, underground, non-ferrous metal ecoinvent 3.3
	CH: treatment of nickel smelter slag, residual material landfill ecoinvent 3.3
	GLO: non-ferrous metal smelter production ecoinvent 3.3
	GLO: treatment of sulfidic tailing, off-site ecoinvent 3.3
	CH: lime production, milled, packed ecoinvent 3.3
	DE: Electricity grid mix ts
	DE: Electricity grid mix ts
	GLO: diesel, burned in building machine ecoinvent 3.3

b. LCIA of heterogeneous catalysts

Life cycle impacts of heterogeneous catalysts in *Bio* scenarios were not available in literature. Therefore, the following considerations/assumptions were made: The Na_2O/SiO_2 dehydration

catalyst is obtained by impregnating a small amount of NaOH on a commercial silica material. Thus Na_2O/SiO_2 was replaced by pure silica for LCIA. Also, the spent material can be considered a non-toxic, general waste once organic residues are burnt off. Thus, no LCA impacts were assigned.

Noble metal catalysts, on the other hand, are sent to a third-party refiner to regain a significant fraction of their metal content after use. For the current analysis, we obtained typical metal loss values (use phase and refining) from the CatCost™ excel tool (v1.0.4, **Table S7**). The remaining metal was assumed to partially cover the required input for catalyst syntheses. Moreover, the support material and catalyst processing steps (synthesis, refining) were neglected in LCIA, due to the expected dominance of metal impacts. Consequently, noble metal catalysts were exclusively represented by the impacts of respective metal losses during a full use cycle (including refining).

Table S7: Data on hydrogenation catalyst use and recycle as extracted from CatCost™.

Material	**Metal Loss (Use)**	**Metal Loss (Recycling)**
Ru/C	5 %	20 %
Pt-Re/TiO_2	10 %	2 %

The impact of Ruthenium production and Platinum production was obtained by economically reallocation of the ecoinvent platinum production process assuming prices and mineral compositions from Nuss et al.[8]

c. iLUC estimations in LCIA

Further LCIA considerations relate to the indirect land use change, which is often associated with first generation biomass feedstocks. To calculate the effect of iLUC on the environmental performance of succinic acid-based NVP, we adapted literature values for indirect land use change provided in the context of biofuel (ethanol) production through sugar fermentation. For this purpose, ethanol production was assumed to return 90% of the theoretical maximum yield. Thus, 3.3 kg of corn, 4.9 kg of corn stover, 14.3 kg of sugar beet, and 15.4 kg of sugar cane are required per kg of ethanol produced. This consideration gives the following iLUC impacts (in terms of GWI) for the four feedstocks of our study related to NVP production for *Bio-Pt-Ex*:

Table S8: iLUC data for corn-based NVP. Adapted from different sources.

	$g_{CO2}\ MJ_{EtOH}^{-1}$	$g_{CO2}\ kg_{corn}^{-1}$	$kg_{CO2}\ kg_{NVP}^{-1}$
EPA RFS2[9]	30	243	0.71
CARB, LCFS[10]	20	160	0.47
Tyner et al.[11]	18	146	0.42
Dunn et al.[12]	8	64	0.19

Table S9: iLUC data for corn-stover-based NVP. Adapted from different sources.

	$g_{CO2}\ MJ_{EtOH}^{-1}$	$g_{CO2}\ kg_{stover}^{-1}$	$kg_{CO2}\ kg_{NVP}^{-1}$
Dunn et al.[12]	-1.21	-6.64	-0.03
Taheripour et al.[13]	-0.97	-5.31	-0.02

Table S10: iLUC data for sugar beet-based NVP. Adapted from different sources.

	$g_{CO2}\ MJ_{EtOH}^{-1}$	$g_{CO2}\ kg_{beet}^{-1}$	$kg_{CO2}\ kg_{NVP}^{-1}$
Al-Riffai et al.[14]	16.07	30.00	0.38
JCR, Eu[15]	5.1	9.52	0.12
IFPRI[16]	5.35	9.99	0.13
Darlington et al.[17]	6	11.20	0.14

Table S11: iLUC data for sugar cane-based NVP. Adapted from different sources.

	g_{CO2} MJ_{EtOH}^{-1}	g_{CO2} kg_{cane}^{-1}	kg_{CO2} kg_{NVP}^{-1}
Al-Riffai 2010[14]	17.78	30.83	0.42
Marelli 2011[15]	14	24.27	0.33
Laborde 2011[16]	15.3	26.53	0.36

5. Process Descriptions

a. GBL-based production

Industrially, NVP is almost exclusively produced through GBL amination and subsequent vinylation of the obtained 2-pyrrolidone (2PYD).[18] Respective models (**Figure S5**) are based on established practices as disclosed in patent literature.[19–21] Accordingly, the amination section of the process features a continuous flow reactor (285 °C, 160 bar) and three downstream distillation columns at variable pressure (15-0.002 bar). In this configuration GBL is efficiently (93.9 mol.%) aminated to 2PYD using a concentrated ammonium hydroxide solution (GBL:NH_3:H_2O =1:2.6:1.9 molar, no catalyst). Subsequently, surplus NH_3 is removed by distillation (15 bar) and recycled. The remaining vacuum columns deal with the removal of (i) wastewater, containing unconverted GBL, and (ii) γ-(*N*-2-pyrrolidonyl)butyramide (NPBY), an undesired amination by-product (4.3 mol.% yield). The resulting 2PYD is partially converted to potassium pyrrolidate (KPYD, 0.05 mol.% of total and 2PYD), the homogeneous vinylation catalyst. A concentrated KOH solution is used, and subsequent water removal (<100 ppm) is essential for an effective conversion to NVP (69 mol.%). The latter proceeds at 20 bar and 150 °C in a batch autoclave. Subsequent removal of surplus acetylene and heavy residue leads to NVP monomer of the desired quality (99 mol.%). In accordance with NVP purification in *Bio* scenarios, vacuum distillation (6.6 mbar) is applied to limit thermal product degradation.[22]

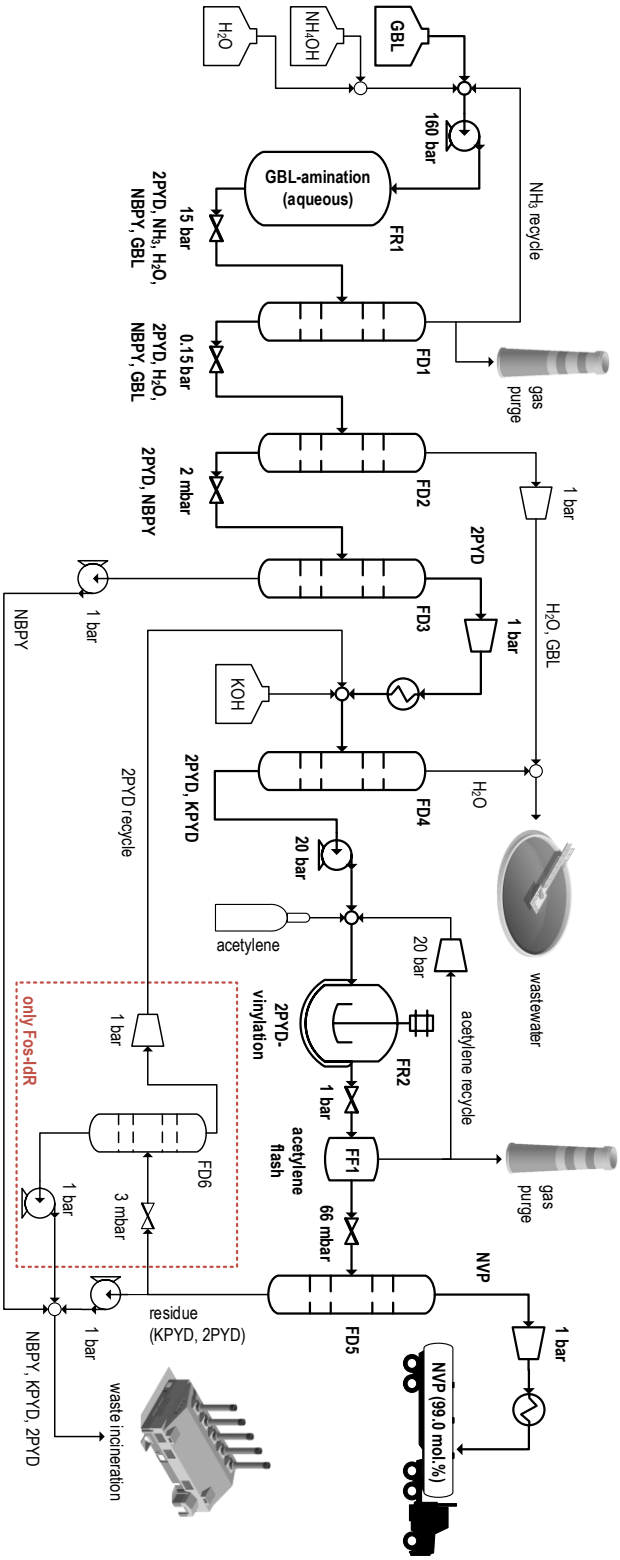

Figure S5: Flowsheet of NVP production from GBL according to the *Fos*/*Fos-IdR* scenarios. Thermolytic treatment of the vinylation residue for 2PYD recovery is adopted from patent literature.[23]

b. Treatment of residues

According to patents used in setting up the *Fos* scenario, the formation of heavy residue comprising e.g., potassium γ-aminobutyrate, limits overall NVP yield in vinylation. Thus, Y(NVP) = 69 mol.% was implemented in the *Fos* model.[21] Since detailed information on the yield and composition of the heavy residue was not available, vinylation side-reactions were not implemented in the corresponding Aspen® *RStoic* model. Instead, 2PYD and KPYD serve as model compounds for heavy-boilers in NVP purification. Within the *Fos* scenario of the main text, these compounds are then sent to waste incineration. Yet, there is some evidence of 2PYD recovery from the heavy residue of vinylation in patent literature.[23] Accordingly, a second scenario (*Fos-IdR*), representing an idealized recovery/recycle of 2PYD from residues, is evaluated in a subsequent section of the supplementary. Here, an additional distillation column (3 mbar) separates 90 % of unconverted 2PYD for recycling. The remainder, together with solid KPYD, is sent to waste incineration. Note that *Fos* and *Fos-IdR* can be considered as limiting cases, with a likely industrial application situated in between.

6. Estimation of Thermodynamic Properties

The accurate evaluation of *RStoic*, *RadFrac* and *Extract* blocks during flowsheet simulation is based on the availability of single component and binary interaction parameters. Most notably, knowledge of the ideal gas heat capacity (c_p^{ig}), the vapor pressure (p_v), the enthalpy of evaporation (ΔH_{vap}), the enthalpy of formation (ΔH_f^0) and NRTL parameters is crucial. Where unavailable from Aspen®-integrated databases, p_v, ΔH_{vap} and NRTL parameters were estimated based on COSMO-RS by using the implementation COSMOthermX17 on the BP-TZVPD-FINE parametrization

(BP-TZVPD-FINE-C30-1701) by COSMOlogic GmbH & Co. KG, Leverkusen, Germany.[24] In the case of p_v, calculated curves were offset by constant values to match literature-known T_B values. Standard enthalpies of formation ΔH_f^0 and heat capacities c_p^{ig} were estimated using the Benson group contribution method[25] as implemented in the estimation tool for thermodynamic data[26] of the reaction mechanism generator. The estimation of NRTL parameters was restricted to the interactions of key components for each separation unit.

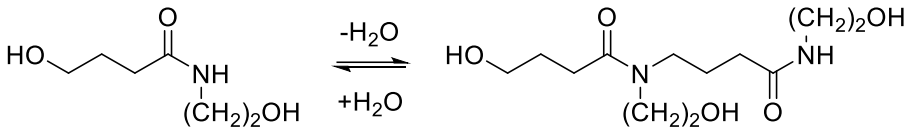

Scheme S1: Dimerization of HEBA (left) to yield DIMER (right) model structure.

For property estimation, the oligomeric species must be represented by a defined model structure. Due to previous insight by Shimasaki et al.[3] and White et al.[4], a DIMER formed from the condensation of two HEBA units (**Scheme S1**) was used for this purpose. The implementation of calculated parameters for the DIMER structure leads to simulated separation behavior (HEP/DIMER) similar to the presented lab-scale experiments. However, the simulated extraction does not lead to complete oligomer removal from HEP, which causes an additional recycle stream in *Bio-x-Ex* (see process flowsheet of the main text). Future research in the continuous separation behavior of amidation-hydrogenation by-products will determine if this is ultimately necessary.

Finally, a summary of all estimated property parameters is given in **Table S12**-**Table S16**. The Aspen® input format is applied throughout.

Table S12: Estimated parameters for the extended Antoine equation (units: K and mbar).

Component	C1	C2	C3
NBPY	16.55	-6069	-83.22
HEP	17.59	-5166	-65.49
N-ethylpyrrolidine	15.33	-2617	-73.99
DIMER	20.90	-11091	-77.23

Table S13: Estimated parameters for the DIPPR 106 equation for the heat of evaporation (units: K and kJ $kmol^{-1}$).

Component	C1	C2	C3	C4	C5	T_C
NBPY	127035	3.144	342.7	-4.712	19907	1E4
HEP	77542	0.251	-0.352	1.557	-1.338	783
N-ethylpyrrolidine	30685	-1.232	2.388	-0.845	-0.268	601
DIMER	140927	-22.10	736.5	-5433	5502	1E4

Table S14: Estimated parameters for the polynomial equation for the ideal gas heat capacity (units: K and kJ $kmol^{-1}$ K^{-1}).

Component	C1	C2	C3	C4	C5
NVP	18.54	0.165	7.361E-4	-1.055E-6	4.208E-10
NBPY	2.203	0.555	3.117E-4	-7.771E-7	3.561E-10
HEP	11.74	0.339	4.310E-4	-7.836E-7	3.324E-10
N-ethylpyrrolidine	14.28	0.181	1.027E-3	-1.472E-6	5.865E-10
DIMER	-45.91	1.871	-2.490E-3	2.008E-6	-6.469E-10

Table S15: Estimated property constants of pure components.

Component	NVP	NBPY	KPYD[a]	HEP	EPINE	DIMER
ΔHf0 [kcal mol-1]	-36.5	-109.4	-101.4	-99.3	-8.7	-252.98

[a] solid.

Table S16: Estimated NRTL parameters for key binary interactions (no units).

I/J	AIJ	AJI	BIJ	BJI	CIJ	DIJ	EIJ	EJI	FIJ	FJI
NVP/2PYD	7.354	2.017	-221.1	44.48	-2.894	-1.373 E-2	-1.193	-0.356	1.199 E-3	4.861 E-4
NVP/H2O[a]	38.92	59.05	-1292	-2867	-1.049	-1.862 E-3	-6.152	-9.070	5.383 E-3	6.509 E-3
NVP/NEP	-666.2	696.9	24175	-24948	-4.219 E-2	1.170 E-3	109.1	-114.1	-0.120	0.126
2PYD/NBPY	2.469	-1.003	-154.9	23.66	-2.274	-4.585 E-3	-0.397	0.179	3.269 E-4	-3.110 E-4
HEP/H2O	85.25	703.7	-4661	-23413	-1.410	-3.784 E-3	-12.55	-117.3	5.062 E-3	0.1434
HEP/DCM	-18.80	59.55	390.9	-2946	-0.427	-4.613 E-3	3.262	-9.515	-4.676 E-3	9.296 E-3
HEP/2PYD	-45.40	-10.85	1270	449.4	11.95	1.999 E-2	7.773	1.727	-1.070 E-2	-1.612 E-3
DIMER/HEP	-0.990	-0.990	215.3	-455.5	0.429	-1.573 E-3	-0.201	-0.642	3.054 E-3	-2.162 E-3
H2O/DIMER	32.10	-96.87	-1044	2344	3.280	2.000 E-2	-5.462	16.86	7.817 E-3	-2.508 E-2
DCM/DIMER	2.247	5.085	-195.0	-314.1	5.705	1.186 E-2	-0.321	-0.668	3.726 E-5	-5.512 E-4

[a] The estimated parameters are used for a description of the water removal from product NVP by distillation. Their applicability for general NVP/H2O mixture prediction is likely limited, due to the prediction of an NVP/H2O-LLE unknown to experimental literature.

7. Operational Cost Analysis

Data for operational cost analysis was derived from the ecoinvent database (v3.7), Aspen® and market/scientific studies. IHS Markit provided cost estimates on some chemicals that were not available elsewhere. Values are given in 2020 USD. Historical inflation and currency conversion factors were applied, where necessary. A summary is given in **Table S17**. Note that data corresponding to Europe (ecoinvent: RER, Eur w/o Ch) was prioritized whenever possible.

Table S17: Data collection used in the estimation of operational cost.

Materials and Energy	Cost	Units	Source
Substrates			
GBL	4.47	$ kg^{-1}	IHS Markit[27]
Succinic acid (base case)	2.50	$ kg^{-1}	weastra/BioConSepT[28]
Succinic acid (optimistic)	1.50	$ kg^{-1}	Morales2016[29]
Ammonia	0.48	$ kg^{-1}	ecoinvent[30]
MEA	1.32	$ kg^{-1}	ecoinvent
Acetylene	1.90	$ kg^{-1}	IHS Markit
Hydrogen	3.89	$ kg^{-1}	ecoinvent
Auxiliaries			
Nitrogen	8.92E-2	$ kg^{-1}	ecoinvent
Process water	3.58E-2	$ kg^{-1}	IHS Markit
DCM	1.42	$ kg^{-1}	ecoinvent
Catalysts			
KOH	0.71	$ kg^{-1}	ecoinvent
Silica	1.36	$ kg^{-1}	ecoinvent
Ru/C[a]	149	$ kg^{-1}	CatCost™ (see below)
Pt-Re/TiO_2[a]	230	$ kg^{-1}	CatCost™ (see below)
Energy			
Natural gas	1.54E-2	$ MJ^{-1}	ecoinvent
Steam	7.77E-3	$ MJ^{-1}	ecoinvent
Refrigeration (-10 °C)	3.00E-2	$ MJ^{-1}	ecoinvent
Cooling water	7.77E-4	$ MJ^{-1}	Aspen®/ecoinvent
Air cooling	0.00	$ MJ^{-1}	Aspen®
Electricity	1.42E-1	$ kWh^{-1}	ecoinvent
In waste treatment			
H_2SO_4 (50 wt.% sol. state)	9.14E-2		ecoinvent
NaOH (15 wt.% sol. state)	2.77E-1		ecoinvent
NaOCl	4.93E-1		ecoinvent
$CuSO_4$	5.47		ecoinvent
NaHS	1.15		ecoinvent

HNO_3 (50 wt.% sol. state)	1.84E-1	ecoinvent
Activated carbon	1.36	ecoinvent
CaO	1.12E-1	ecoinvent
HCl (30 wt.% sol. state)	1.84E-1	ecoinvent
Light fuel oil	3.89E-1	ecoinvent

[a] The given cost corresponds to the use phase only. The sales price of spent material was deducted.

Again, data on heterogeneous catalysts within *Bio* scenarios for NVP production had to be approximated. As in LCIA, the Na_2O/SiO_2 catalyst was replaced by pure silica for this purpose. Prices of hydrogenation catalysts, on the other hand, were approximated by the market price of metals (**Table S18**) lost during use and refining plus refining fees (**Table S19**). The latter were obtained from CatCost^{TM}.

Table S18: Spot prices of metals for catalyst synthesis (retrieved: 26.10.2020).

Metal	**Spot Price [$ kg^{-1}]**	**Source**
Ru	9,800	[31]
Pt	31,500	[31]
Re[a]	1,500	[32]

[a] Re markets have been volatile over past years so that significantly different price estimates are possible.

Table S19: Data on hydrogenation catalyst use and recycle as extracted from CatCost^{TM}.

Material	**Cost of Lost Metal [$ kg$_{Cat}^{-1}$]**	**Recycling Cost [$ kg$_{Cat}^{-1}$]**
Ru/C	118	32
Pt-Re/TiO_2	204	26

8. Exemplary Comparison of Unit Operations (*Fos-IdR* vs. *Bio-Pt-Ex*)

While an estimation of capital expenditure is beyond the scope of the analysis, an exemplary comparison of unit operations for NVP production from succinic acid and GBL is given in **Table S20** and **Table S21**. Each piece of equipment is characterized by p-/T-conditions as well as normalized throughput (per FU) from the equilibrium simulations. Notably, a similar number and type of vessels is required for both value chains.

Table S20: Specifications of reactors and separation units in *Bio-Pt-Ex*.

Equipment for *Bio-Pt-Ex*			
Reactors			
BR1 – Amidation-Hydrogenation		**BR2** - Dehydration	
Pressure [bar]:	200	Pressure [bar]:	1
Temperature [°C]:	200	Temperature [°C]:	385
Mode:	batch	Mode:	continuous
Phases:	gas/liquid	Phases:	gas
Flow [kg kg_{NVP}^{-1}]:	4.0	Flow [kg kg_{NVP}^{-1}]:	3.8
Flash separators			
BF1 - Hydrogen		**BF2** - Nitrogen	
Pressure [bar]:	180	Pressure [bar]:	1
Temperature [°C]:	102	Temperature [°C]:	20
Gas flow [kg kg_{NVP}^{-1}]:	0.5	Gas flow [kg kg_{NVP}^{-1}]:	2.6
Liq. flow [kg kg_{NVP}^{-1}]:	3.5	Liq. flow [kg kg_{NVP}^{-1}]:	1.2
Columns			
BE1 – Extraction		**BD3** – DCM distillation	
Plates (theo.)	6	Plates (theo.)	6
Pressure [bar]:	1	Pressure [bar]:	1
T_Ex. [°C]:	20	T_Head [°C]:	38
T_Ret [°C]:	20	T_Bottoms [°C]:	245
Ex. [kg kg_{NVP}^{-1}]:	8.1	Head [kg kg_{NVP}^{-1}]:	6.7
Ret. [kg kg_{NVP}^{-1}]:	2.3	Bottoms [kg kg_{NVP}^{-1}]:	1.4

BD4 – Light by-product dist.		**BD5** – HEP distillation	
Plates (theo.)	10	Plates (theo.)	6
Pressure [bar]:	1	Pressure [bar]:	1
T_Head [°C]:	128	T_Head [°C]:	277
T_Bottoms [°C]:	277	T_Bottoms [°C]:	282
Head [kg kg_{NVP}^{-1}]:	0.04	Head [kg kg_{NVP}^{-1}]:	1.3
Bottoms [kg kg_{NVP}^{-1}]:	1.36	Bottoms [kg kg_{NVP}^{-1}]:	0.1
BD6 – Light by-product dist.		**BD7** – HEP distillation	
Plates (theo.)	8	Plates (theo.)	6
Pressure [bar]:	0,199	Pressure [bar]:	0,066
T_Head [°C]:	60	T_Head [°C]:	108
T_Bottoms [°C]:	141	T_Bottoms [°C]:	160
Head [kg kg_{NVP}^{-1}]:	0.2	Head [kg kg_{NVP}^{-1}]:	1.0
Bottoms [kg kg_{NVP}^{-1}]:	1.0	Bottoms [kg kg_{NVP}^{-1}]:	0.05

Table S21: Specifications of reactors and separation units in *Fos-IdR*.

Equipment for *Fos-IdR*			
Reactors			
FR1 - Amination		**FR2** - Vinylation	
Pressure [bar]:	160	Pressure [bar]:	20
Temperature [°C]:	285	Temperature [°C]:	150
Mode:	continuous	Mode:	batch
Phases:	liquid	Phases:	gas/liquid
Flow [kg kg_{NVP}^{-1}]:	1.7	Flow [kg kg_{NVP}^{-1}]:	4.5
Flash separators			
FF1 - Acetylene			
Pressure [bar]:	1		
Temperature [°C]:	22		
Gas flow [kg kg_{NVP}^{-1}]:	3.2		
Liq. flow [kg kg_{NVP}^{-1}]:	1.4		

Columns

FD1 – NH_3 distillation		**FD2** – Wastewater distillation	
Plates (theo.)	20	Plates (theo.)	6
Pressure [bar]:	15	Pressure [bar]:	0,15
T_Head [°C]:	39	T_Head [°C]:	65
T_Bottoms [°C]:	211	T_Bottoms [°C]:	185
Head [kg kg_{NVP}^{-1}]:	0.3	Head [kg kg_{NVP}^{-1}]:	0.5
Bottoms [kg kg_{NVP}^{-1}]:	1.4	Bottoms [kg kg_{NVP}^{-1}]:	0.9

FD3 – 2PYD distillation		**FD4** – Drying column	
Plates (theo.)	6	Plates (theo.)	10
Pressure [bar]:	0,002	Pressure [bar]:	1
T_Head [°C]:	90	T_Head [°C]:	100
T_Bottoms [°C]:	128	T_Bottoms [°C]:	250
Head [kg kg_{NVP}^{-1}]:	0.8	Head [kg kg_{NVP}^{-1}]:	0.02
Bottoms [kg kg_{NVP}^{-1}]:	0.1	Bottoms [kg kg_{NVP}^{-1}]:	1.1

FD5 – NVP distillation		**FD6** – Residue recycle column	
Plates (theo.)	12	Plates (theo.)	6
Pressure [bar]:	0.066	Pressure [bar]:	0.003
T_Head [°C]:	107	T_Head [°C]:	- (96)[a]
T_Bottoms [°C]:	158	T_Bottoms [°C]:	- (96)
Head [kg kg_{NVP}^{-1}]:	1.0	Head [kg kg_{NVP}^{-1}]:	0.3
Bottoms [kg kg_{NVP}^{-1}]:	0.4	Bottoms [kg kg_{NVP}^{-1}]:	0.1

[a] boiling point of 2PYD, since chemical composition of vinylation residue is mostly undefined;

9. Analysis of Alternative Scenarios for Fossil-Based NVP Production (*Fos-IdR*)

Table S22: LCI data for GBL-based production models. Options with (*Fos-IdR*) and without (*Fos*, see main text) recovery of 2PYD from the vinylation residue are compared.

Production Scenario:	***Fos***	***Fos-IdR***	
Stream	**Quantity (normalized to FU)**		**units**
Chemicals			
γ-Butyrolactone	1.23	0.90	kg kg_{NVP}^{-1}
Ammonia	0.26	0.19	kg kg_{NVP}^{-1}
Process water	0.50	0.37	kg kg_{NVP}^{-1}
Acetylene	0.28	0.016	kg kg_{NVP}^{-1}
KOH	0.016	0.28	kg kg_{NVP}^{-1}
Utilities			
Natural gas	1.67	1.26	MJ kg_{NVP}^{-1}
Steam	2.23	1.80	MJ kg_{NVP}^{-1}
Cryogen[a]	1.10	1.09	MJ kg_{NVP}^{-1}
Water cooling	1.40	1.10	MJ kg_{NVP}^{-1}
Air cooling	5.28	4.74	MJ kg_{NVP}^{-1}
Electricity	0.79	0.74	kWh kg_{NVP}^{-1}
(Total exergy)[b]	(4.82)	(4.26)	MJ kg_{NVP}^{-1}
Waste[c]			
Inert gas purge	-	-	kg kg_{NVP}^{-1}
Flam. gas purge	0.05	0.05	kg kg_{NVP}^{-1}
Organic residue	0.46	0.13	kg kg_{NVP}^{-1}
Wastewater	0.78	0.57	kg kg_{NVP}^{-1}

Section 5.a of this supplementary describes a modification of the *Fos* scenario with idealized recycling of vinylation residues (*Fos-IdR*). LCI data of both scenarios, *Fos* and *Fos-IdR*, is compared in **Table S22**. As expected, the *Fos-IdR* model has significantly reduced requirements for substrates and energy per functional unit. These savings are due to the increased overall yield of NVP from GBL (86 mol.%), which is not fully counterbalanced by the energy input for an

additional separation of 2PYD from the vinylation residue. Likewise, the amount of waste organics is reduced due to the lowered quantity of residues sent to waste incineration.

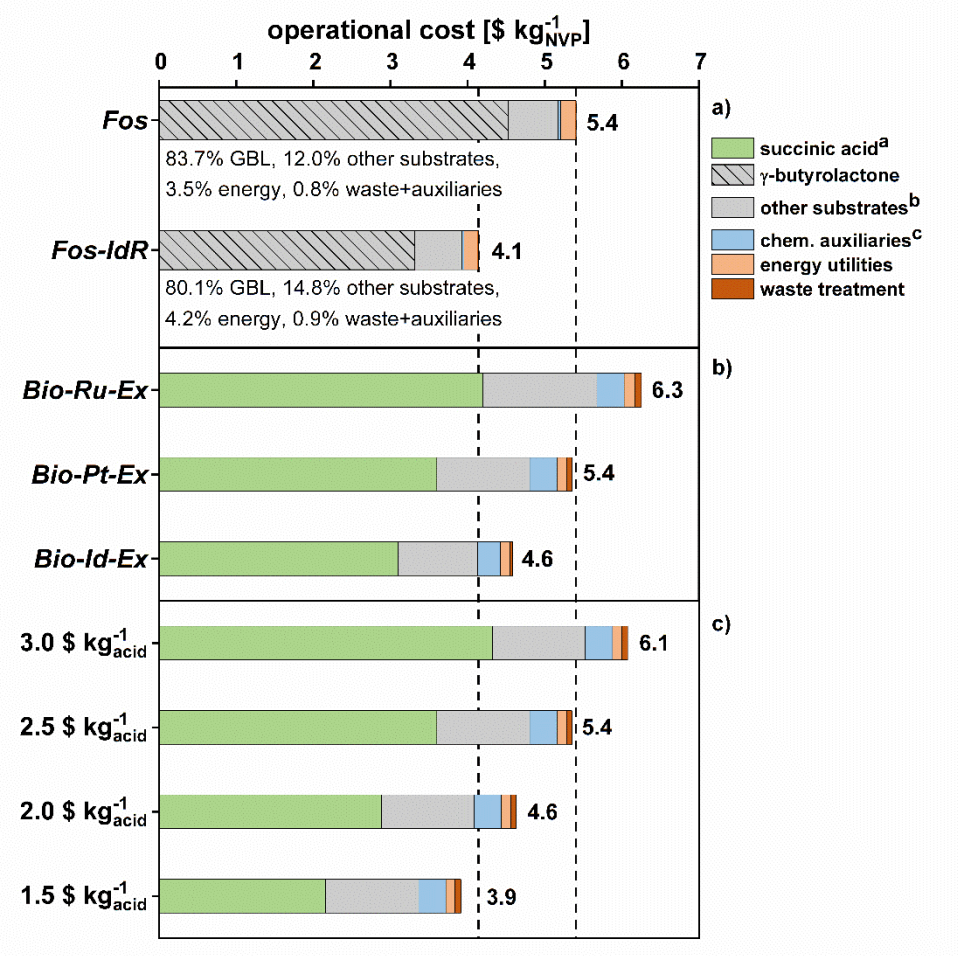

Figure S6: Operational cost in NVP production depending on a) recycling assumptions, b) catalyst technology and c) substrate cost in *Bio-Pt-Ex*. 2.5 \$ kg_{Acid}^{-1} unless specified otherwise. [a]Succinic acid is derived from sugar beet, [b] other substrates include H_2 and monoethanolamine (*Bio*) as well as ammonia and acetylene (*Fos*), [c] catalysts (heterogeneous and KOH), solvents (H_2O, DCM) and inerts (N_2) are summarized as auxiliaries;

Naturally, the discussed changes in the LCI have a pronounced impact on operational cost estimates. Thus, the idealized *Fos-IdR* scenario operates at 76 % (4.1 \$ kg_{NVP}^{-1}) of the cost of fossil NVP production without 2PYD recycle (**Figure S6**). Consequently, even an idealized catalyst would not allow for a competitive cost structure of the *Bio* scenario (*Bio-Id-Ex*) given the assumed

market conditions (2.5 \$ kg_{Acid}^{-1}). For the best currently achievable option (*Bio-Pt-Ex*) operational costs on the level of *Fos-IdR* result for a substrate price of 1.7 \$ kg_{Acid}^{-1} – relating to a price ratio (succinic acid/GBL) of 0.45. Notably, this may be within the reach of newly developed technologies.[29] Moreover, given the cited patent literature, a realistic scenario for fossil-based NVP production is likely to fall in between *Fos* and *Fos-IdR*.[19–21]

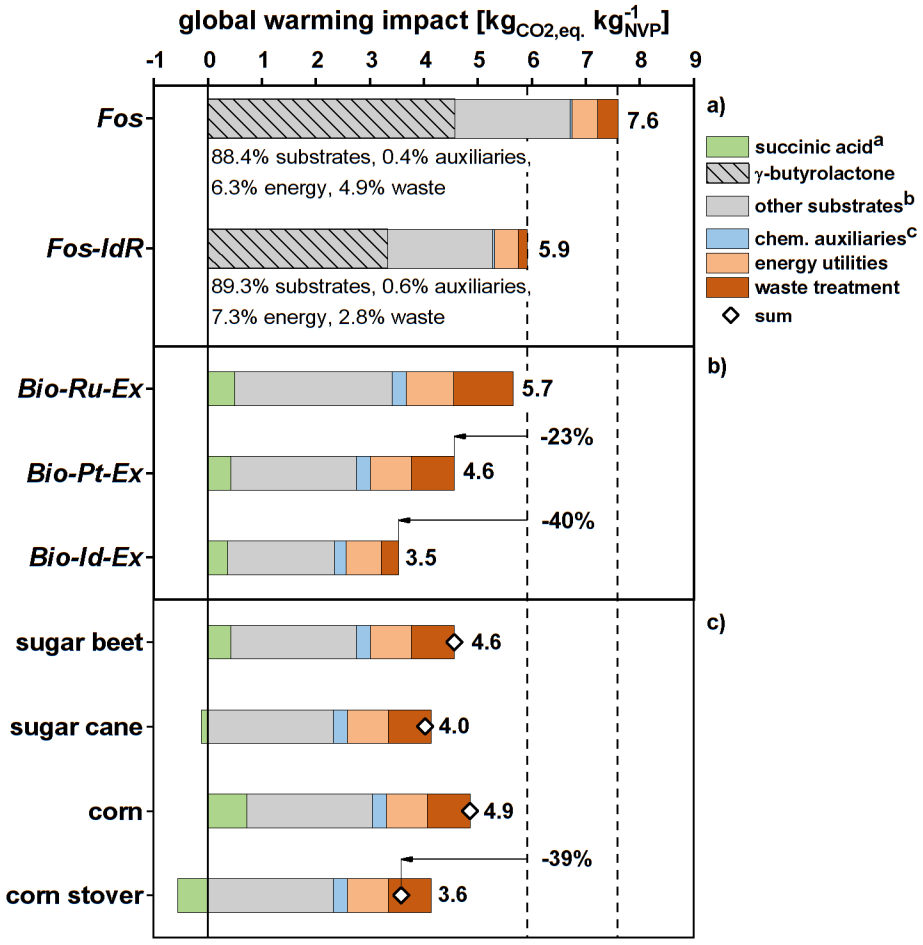

Figure S7: Global warming impact of NVP production as a function of a) recycling assumptions, b) catalyst technology and c) fermentation feedstock in *Bio-Pt-Ex*. [a]Succinic acid is derived from sugar beet unless specified otherwise, [b] other substrates include H_2 and monoethanolamine (*Bio*) as well as ammonia and acetylene (*Fos*), [c] catalysts (heterogeneous and KOH), solvents (H_2O, DCM) and inerts (N_2) are summarized as auxiliaries;

The global warming impact of the *Fos-IdR* scenario is 22 % (relative) below that of the original *Fos* scenario (**Figure S7**). The reasons lie within the LCI changes, whose impact on operational costs was discussed above. Still, the *Bio-Pt-Ex* scenario reduces GWI compared to *Fos-IdR* by 23 %. Further improvements of the catalyst system would allow for a cut of global warming impacts by 40 % with respect to *Fos-IdR*. Similarly, the use of sugar from corn stover for succinic acid production would allow for a more favorable *Bio-Pt-Ex* scenario (39 % relative GWI reduction). Overall, the GWI benefit of *Bio* scenarios is thus much more robust with respect to process assumptions than their economic feasibility.

10. Detailed Waste Stream Compositions and LCIs

The evaluation of waste stream treatment is based on previously published analysis of industrial plants. These provide general consumption and emission factors related to the volume and composition of each waste stream. For example, 287 kWh of electricity are allocated to the incineration of 1 t of waste solvent (organic), whereas NaOH consumption depends on chloride content.[33] Thus, necessary details on waste stream composition are summarized below (**Table S23**-**Table S25**).

Table S23: Composition (kg kg^{-1}) of flammable purge gas from different process models.

Component	***Fos***	***Fos-IdR***	***Bio-Ru-D***	***Bio-Ru-Ex***	***Bio-Pt-Ex***	***Bio-Id-Ex***
Acteylene	0.791	0.833	-	-		-
NVP	0.016	0.017	-	-		-
Ammonia	0.191	0.149	-	-		-
Hydrogen	-	-	0.511	0.511	0.454	0.584
Methane	-	-	0.366	0.365	0.098	0.000
Ethane	-	-	0.095	0.095	0.424	0.384

Water	0.002	0.002	0.028	0.028	0.024	0.031

Table S24: Composition (kg kg^{-1}) of waste organics for incineration from different process models.

Component	***Fos***	***Fos-IdR***	***Bio-Ru-D***	***Bio-Ru-Ex***	***Bio-Pt-Ex***	***Bio-Id-Ex***
NVP	0.004	0.015	0.005	0.009	0.011	0.018
NBPY	0.160	0.408	-	-	-	-
KPYD	0.076	0.262	-	-	-	-
DCM	-	-	-	0.228	0.229	0.293
HEP	-	-	0.204	0.184	0.228	0.450
N-ethyl-…	-	-	0.000	0.087	0.122	0.000
N-methyl-…	-	-	0.000	0.107	0.011	0.000
2-pyrrolidone	0.760	0.315	0.056	0.112	0.147	0.204
N-ethylpyrrolidine	-	-	0.000	0.028	0.000	0.000
GBL	-	-	0.000	0.066	0.000	0.000
1,4-butanediol	-	-	0.006	0.082	0.128	0.022
Succinic acid	-	--	0.000	0.000	0.029	0.000
Butyric acid	-	-	0.000	0.028	0.072	0.000
Propionic acid	-	-	0.000	0.042	0.000	0.000
MEA	-	-	0.000	0.026	0.022	0.000
DIMER	-	-	0.729	0.002	0.001	0.012

Table S25: Composition (kg kg^{-1}) of wastewater from different process models.

Component	***Fos***	***Fos-IdR***	***Bio-Ru-D***	***Bio-Ru-Ex***	***Bio-Pt-Ex***	***Bio-Id-Ex***
NVP	-	-	0.010	0.010	0.012	0.014
DCM	-	-	0.000	0.018	0.017	0.016
HEP	-	-	0.005	0.009	0.011	0.012
N-ethyl-…	-	-	0.011	0.004	0.006	0.000
N-methyl-…	-	-	0.028	0.018	0.002	0.000
2-pyrrolidone	0.005	0.005	0.002	0.001	0.002	0.002
N-ethylpyrrolidine	-	-	0.003	0.001	0.000	0.000
GBL	0.002	0.001	0.005	0.000	0.000	0.000
1,4-butanediol	-	-	0.006	0.000	0.000	0.000
Succinic acid	-	-	0.000	0.000	0.002	0.000

Butyric acid	-	-	0.002	0.000	0.000	0.000
Propionic acid	-	-	0.005	0.002	0.000	0.000
MEA	-	-	0.013	0.010	0.010	0.000
DIMER	-	-	0.000	0.092	0.054	0.013
Ammonia	0.005	0.005	-	-		-
Acetaldehyde	-	-	0.003	0.003	0.004	0.005
Water	0.989	0.989	0.906	0.831	0.879	0.937

This data was evaluated adhering to the schemes of earlier studies.[33,34] In this context, waste organics were burnt in an incineration plant, recovering a fraction of their calorific value.[33] The addition of flammable gases purged from the process increased the average waste heating value and thus reduced the need for co-feeding light fuel oil. Wastewater was treated in a sequence of wet air oxidation and mechanical-biological treatment facilities.[34] Exemplary LCIs and emission values are given in **Table S26**.

Table S26: LCI and emission data for waste treatment in exemplary *Fos* and *Bio* scenarios.

Materials and Energy	***Fos-IdR***	***Bio-Pt-Ex***	**Units**
Auxiliary chemicals			
Activated carbon	8.0E-6	5.69E-4	kg kg_{NVP}^{-1}
CaO	2.8E-4	1.26E-3	kg kg_{NVP}^{-1}
$CuSO_4$	2.1E-5	9.2E-5	kg kg_{NVP}^{-1}
HCl (32 wt.% sol. state)	3.3E-4	4.4E-4	kg kg_{NVP}^{-1}
HNO_3 (50 wt.% sol. state)	5.3E-4	2.4E-3	kg kg_{NVP}^{-1}
H_2SO_4 (96 wt.%)	7.4E-3	3.3E-2	kg kg_{NVP}^{-1}
NaHS (30 wt.% sol. state)	1.9E-5	8.7E-5	kg kg_{NVP}^{-1}
NaOCl (14 wt.% sol. state)	3.0E-5	1.3E-4	kg kg_{NVP}^{-1}
NaOH (50 wt.% sol. state)	1.1E-2	7.7E-2	kg kg_{NVP}^{-1}
NH_3 (25 wt.% sol. state)	1.2E-3	1.1E-3	kg kg_{NVP}^{-1}
Process water	2.4E-3	2.7E-2	kg kg_{NVP}^{-1}
Energy			
Natural gas	0.156	0.254	MJ kg_{NVP}^{-1}

Steam	0.000[a]	0.000[a]	MJ kg_{NVP}^{-1}
Cooling water	0.042	2.032	MJ kg_{NVP}^{-1}
Electricity	0.042	0.266	kWh kg_{NVP}^{-1}
Emissions (to air)			
CO	2.9E-6	3.9E-6	kg kg_{NVP}^{-1}
CO_2	3.9E-1	8.5E-1	kg kg_{NVP}^{-1}
HCl	0.000	4.6E-4	kg kg_{NVP}^{-1}
N_2	2.7E-2	3.2E-2	kg kg_{NVP}^{-1}
NH_3	3.2E-5	1.7E-5	kg kg_{NVP}^{-1}
NMVOC	3.9E-7	5.3E-7	kg kg_{NVP}^{-1}
NO_2	7.2E-4	3.9E-4	kg kg_{NVP}^{-1}
Emissions (to water)			
C (organic, aq.)	3.5E-5	2.5E-3	kg kg_{NVP}^{-1}
CH_2Cl_2 (aq.)	0.000	2.3E-3	kg kg_{NVP}^{-1}
Cl^- (aq.)	0.000	6.8E-2	kg kg_{NVP}^{-1}
K^+ (aq.)	1.1E-2	0.000	kg kg_{NVP}^{-1}
NH_4^+ (aq.)	3.8E-4	4.2E-3	kg kg_{NVP}^{-1}
NO_3^- (aq.)	3.3E-4	3.6E-3	kg kg_{NVP}^{-1}
NO_2^- (aq.)	1.2E-5	1.3E-4	kg kg_{NVP}^{-1}

[a] steam requirements were met with steam from the incineration of organic waste streams.

11. Tabulated LCA Results

Table S27: Tabulated environmental impacts.

	Fos	*Fos-IdR*	*Bio-Ru-D*	*Bio-Ru-Ex*	*Bio-Pt-Ex*	*Bio-Id-Ex*	*Bio-Pt-Ex* (Corn)	*Bio-Pt-Ex* (Beet)*t*	*Bio-Pt-Ex* (Cane)	*Bio-Pt-Ex* (Stover)	*Bio-Pt-Ex* (Adom)	*Bio-Pt-Ex* (Cok Id)
Abiotic Depletion elements [kg$_{Sb\ eq.}$]	3.37E-06	3.20E-06	1.21E-05	1.38E-05	2.11E-05	1.79E-05	1.92E-05	2.11E-05	1.89E-05	1.89E-05	2.1E-05	2.1E-05
Abiotic Depletion fossil [MJ]	1.24E+02	1.03E+02	1.08E+02	1.12E+02	9.66E+01	8.27E+01	9.82E+01	9.66E+01	8.89E+01	8.54E+01	1.1E+02	9.399E+01
Acidification Potential [kg$_{SO2\ eq.}$]	1.19E-02	9.49E-03	4.85E-02	4.77E-02	9.42E-02	8.01E-02	9.42E-02	9.42E-02	9.18E-02	8.94E-02	9.6E-02	9.313E-02
Eutrophication Potential [kg$_{Phosphate\ eq.}$]	1.65E-03	1.04E-03	4.71E-03	5.94E-03	4.29E-03	2.74E-03	6.59E-03	4.29E-03	1.09E-02	2.86E-03	4.8E-03	3.957E-03
Freshwater Aquatic Ecotox. Pot. [kg$_{DCB\ eq.}$]	5.60E-02	5.71E-02	2.33E-01	2.29E-01	4.02E-01	3.43E-01	3.81E-01	4.02E-01	3.96E-01	3.40E-01	4.3E-01	3.881E-01
Global Warming Potential [kg$_{CO2\ eq.}$]	7.60E+00	5.92E+00	5.31E+00	5.66E+00	4.57E+00	3.54E+00	4.86E+00	4.57E+00	4.02E+00	6.39E+00	5.07E+00	4.334E+00
Global Warming excl bio [kg$_{CO2\ eq.}$]	7.60E+00	5.92E+00	7.96E+00	8.25E+00	6.79E+00	5.45E+00	6.99E+00	6.79E+00	6.17E+00	5.68E+00	7.3E+00	6.540E+00
Human Toxicity Pot. [kg$_{DCB\ eq.}$]	2.63E-01	2.32E-01	4.44E-01	4.54E-01	4.86E-01	4.13E-01	4.24E-01	4.86E-01	4.42E-01	2.66E-01	5.6E-01	4.349E-01
Marine Aquatic Ecotoxicity Pot. [kg$_{DCB\ eq.}$]	3.27E+02	2.89E+02	6.75E+02	6.96E+02	8.24E+02	6.93E+02	7.24E+02	8.24E+02	7.71E+02	5.60E+02	8.8E+02	7.625E+02
Ozone Layer Depletion Pot. [kg$_{R11\ eq.}$]	3.05E-09	3.81E-09	1.56E-09	1.53E-09	3.55E-09	3.02E-09	3.60E-09	3.55E-09	3.61E-09	3.56E-09	3.5E-09	3.553E-09
Photochem. Ozone Creation Pot. [kg$_{Ethene\ eq.}$]	7.10E-03	5.25E-03	2.48E-03	2.46E-03	4.25E-03	3.61E-03	4.31E-03	4.25E-03	4.17E-03	3.95E-03	4.4E-03	4.182E-03
Terrestric Ecotoxicity Potential [kg$_{DCB\ eq.}$]	1.19E-02	9.75E-03	1.05E-02	1.09E-02	9.73E-03	8.30E-03	9.44E-03	9.73E-03	9.11E-03	9.05E-03	9.0E-03	9.571E-03

12. ABBREVIATIONS

HEP, *N*-(2-hydroxyethyl)-2-pyrrolidone; NMP, *N*-methyl-2-pyrrolidone; 2PYD, 2-pyrrolidone; GBL, γ-butyrolactone; MEA, monoethanolamine; TMSCl, trimethylsilyl chloride; NEP, *N*-ethyl-2-pyrrolidone; BSTFA, *N,O*-bis(trimethylsilyl)trifluoroacetamide; DCM, dichloromethane; HEBA, *N*-(2-hydroxyethyl)-4-hydroxybutanamide; LCI, life cycle inventory; LCIA, life cycle impact assessment; iLUC, indirect land-use change; NBPY, γ-(*N*-2-pyrrolidonyl)butyramide; KPYD, potassium pyrrolidate; COSMO-RS, conductor-like screening model for realistic solvation; NRTL, non-random two liquids; DIMER, dimer model structure; EPINE, *N*-ethyl-2-pyrrolidine; LLE, liquid-liquid equilibrium; GWI, global warming impact;

13. References

1 M. O. Haus et al., *ACS Catal.*, 2021, **11**, 5119–5134.

2 M. O. Haus et al., *Green Chem.*, 2019, **21**, 6268–6276.

3 Y. Shimasaki et al., *BCSJ*, 2008, **81**, 449–459.

4 J. F. White et al., *Top Catal*, 2014, **57**, 1325–1334.

5 B. Winter et al., *Journal of Cleaner Production*, 2021, **290**, 125818.

6 B. Cok et al., *Biofuels, Bioprod. Bioref.*, 2014, **8**, 16–29.

7 D. J. Lundberg et al., *ACS Sustainable Chem. Eng.*, 2019, **7**, 5576–5586.

8 P. Nuss and M. J. Eckelman, *PloS one*, 2014, **9**, e101298.

9 A. Broch et al., *Environmental Science & Policy*, 2013, **29**, 147–157.

10 California Air Resources Board, *LCFS Land Use Change Assessment,* available at: https://ww2.arb.ca.gov/resources/documents/lcfs-land-use-change-assessment, accessed 17 October 2021.

11 W. E. Tyner et al., *Land Use Changes and Consequent CO2 Emissions due to US Corn Ethanol*, Purdue University, 2010.

12 J. B. Dunn et al., *Biotechnology for biofuels*, 2013, **6**, 51.

13 F. Taheripour and W. E. Tyner, *Economics Research International*, 2013.

14 P. Al-Riffai et al., *Global trade and environmental impact study of the EU biofuels mandate*, 2010.

15 L. Marelli et al., *Estimate of GHG emissions from global land use change scenarios*, 2011.

16 D. Laborde Debucquet, *Assessing the land use change consequences of European biofuel policies*, 2011.

17 T. Darlington et al., *Land Use Change Greenhouse Gas Emissions of European Biofuel Policies Utilizing the Global Trade Analysis Project (GTAP) Model*, 2013.

18 A. L. Harreus et al., in *Ullmann's Encyclopedia of Industrial Chemistry*, Wiley-VCH Verlag GmbH & Co. KGaA, Weinheim, Germany, 2000.

19 M. Rudloff et al. BASF AG, US *Pat.*, 7164031B2, 2007.

20 R. Vogelsang et al. BASF SE, WO *Pat.*, 2009074534A1, 2009.

21 W. Staffel et al. BASF SE, WO *Pat.*, 2009071479A1, 2009.

22 Y. Yamaguchi et al. Nippon Shokubai Co. Ltd., EP *Pat.*, 1094061B2, 2001.

23 H. Helfert et al. BASF AG, WO *Pat.*, 2001085682A1, 2001.

24 A. Klamt et al., *Annual review of chemical and biomolecular engineering*, 2010, **1**, 101–122.

25 S. W. Benson, *Thermochemical kinetics*, Wiley, 1976.

26 G. R. Magoon and W. H. Green, *Computers & Chemical Engineering*, 2013, **52**, 35–45.

27 IHS Markit, *Chemical Economics Handbook*, 2017.

28 weastra s.r.o., *WP 8.1. Determination of market potential for selected platform chemicals,* available at: https://www.cbp.fraunhofer.de/content/dam/cbp/en/documents/project-reports/BioConSepT_Market-potential-for-selected-platform-chemicals_report1.pdf, accessed 13 October 2021.

29 M. Morales et al., *Energy Environ. Sci.*, 2016, **9**, 2794–2805.

30 G. Wernet et al., *Int J Life Cycle Assessment*, 2016, **21**, 1218–1230.

31 MetalsDaily, *Live PGM Prices,* available at: https://www.metalsdaily.com/live-prices/pgms/, accessed 26 October 2020.

32 Kitco, *Strategic Metals,* available at: https://www.kitco.com/strategic-metals/, accessed 26 October 2020.

33 C. Seyler et al., *Journal of Cleaner Production*, 2005, **13**, 1211–1224.

34 A. Köhler, PhD Thesis, ETH Zurich, 2006.

35 F. Adom, J. B. Dunn, J. Han and N. Sather, *Environ. Sci. Technol.*, 2014, **48**, 14624-14631.